Mathematical Biosciences and Engineering

https://www.aimspress.com/journal/mbe

MBE, 22(8): 2152–2175.
DOI: 10.3934/mbe.2025079
Received: 25 March 2025
Revised: 22 May 2025
Accepted: 17 June 2025
Published: 04 July 2025

Research article

Stable periodic solutions of a delayed reaction-diffusion model of Hes1-mRNA interactions

Mohammed Alanazi[1], **Majid Bani-Yaghoub**[1,*] **and Bi-Botti C. Youan**[2]

[1] Division of Computing, Analytics & Mathematics, School of Science and Engineering, University of Missouri-Kansas City, 5100 Rockhill Rd., Kansas City, Missouri 64110, USA

[2] Laboratory of Future Nanomedicines and Theoretical Chronopharmaceutics, Division of Pharmaceutical Sciences, School of Pharmacy, University of Missouri-Kansas City, 2464 Charlotte Street, Kansas City, Missouri 64108, USA

* **Correspondence:** Email: baniyaghoubm@umkc.edu.

Abstract: Hes1 (Hairy and enhancer of split 1) is a transcriptional repressor that plays a fundamental role in the regulation of embryogenesis and cell lineage specification. The temporal dynamics of Hes1 mRNA and Hes1 protein expression are known to exhibit sustained oscillations. However, many existing mathematical models can reproduce these oscillations only transiently, eventually dampening toward a steady state. This limits their biological fidelity, as sustained oscillations are observed in vitro and in vivo under physiological conditions. To address these limitations, we propose a more biologically realistic framework by incorporating both transcriptional/translational time delays and spatial diffusion effects into a Reaction-Diffusion (RD) system with discrete time delays. The model describes the spatiotemporal dynamics of Hes1 mRNA and protein concentrations in the cytoplasm and nucleus. We establish the conditions under which the RD model undergoes a delay-induced Hopf bifurcation, leading to the emergence of stable periodic solutions. Furthermore, our analysis establishes explicit criteria on the delay and diffusion coefficients that ensure the existence of sustained oscillatory patterns. Numerical simulations are conducted to validate the theoretical predictions, demonstrating the persistence and stability of oscillations under a range of biologically plausible parameters.

Keywords: Hes1-mRNA interaction; periodic solutions; bifurcation analysis; reaction-diffusion model

1. Introduction

The Hes1 gene is part of a family of mammalian genes, homologous to the Drosophila genes hairy and enhancer of split [1–3]. It encodes a transcriptional repressor that belongs to the basic helix-

loop-helix (bHLH) family of transcription factors. As one of the seven members of the Hes gene family (HES1-7), Hes1 is crucial in controlling cell proliferation and differentiation during embryogenesis [4, 5]. The Hes1 protein is a nuclear repressor, a type of transcription factor that inhibits the expression of target genes by blocking the binding of bHLH activators to DNA [6,7]. A significant feature of its regulation is its ability to regulate its own expression through a negative feedback loop [8]. Messenger RNA (mRNA) is pivotal in the gene expression process, serving as a single-stranded intermediary molecule that conveys genetic information from the DNA in the nucleus to the cytoplasm. In the cytoplasm, the mRNA sequence is translated into a corresponding protein, with each three-base codon specifying an amino acid that is sequentially assembled into a polypeptide chain [9, 10]. Thus, transcription of the Hes1 gene and subsequent translation of its mRNA are integral steps in the production of the Hes1 protein [8, 11].

Periodic behavior is a fundamental characteristic of the regulatory system of Hes1-mRNA. Based on experimental data from [12], researchers have observed that Hes1-mRNA interactions exhibit oscillatory behavior with a period of approximately two hours. To simulate this oscillatory behavior, a model was developed [12] using a three-dimensional system of ordinary differential equations (ODE), which included variables representing Hes1 protein, Hes1 mRNA, and an additional Hes1-interacting factor. Although this model successfully reproduced the observed two-hour period, it relied on an unknown variable (the Hes1 interacting factor) to achieve oscillations consistent with the experimental data. To address the issue of this unknown variable, subsequent models incorporated a delay term into the model, as described in [13] and [14], thus eliminating the need for the third variable. The simplified delay model in [14] captures the essential oscillatory dynamics observed in autoregulatory genes such as Hes1, which functions as its inhibitor. This model consists of two equations: one that governs the rate of change of mRNA levels, which carry genetic information to the ribosome for protein synthesis, and another that governs the rate of change in protein concentration. In this system, mRNA levels are regulated by the Hes1 protein with a delay that accounts for transcriptional and translational processes. The delay arises from the series of biological processes that start with the transcription of the Hes1 gene into mRNA and continue until the first Hes1 protein inhibits further transcription of the Hes1 gene. To represent this regulation, a Hill function [15] with a delay term was employed, simplifying the complex biological interactions.

Several modeling approaches have attempted to more accurately reflect the cyclic behavior of Hes1 expression and align with experimental data. Notably, experimental observations indicate that Hes1 expression does not exhibit an overshoot when initiated, a feature likely attributed to biological complexity. A recent study addressed this overshooting issue by modifying the existing delay differential equation (DDE) model to account for Gro protein interactions [16]. Furthermore, while previous models often incorporated discrete delays, biological systems exhibit continuous variability in delays. To accommodate this, [17] extended the model by incorporating a distributed time delay, better reflecting natural biological variability. Moreover, experimental data indicate that the amplitude of Hes1 oscillations in mouse cells is higher than what simple Hes1-mRNA models predict [18]. To address this discrepancy, researchers have expanded DDE models to include processes such as nucleo-cytoplasmic transport, the formation of Hes1 monomers and dimers, and differences in their stability. These extensions have improved the model's ability to capture the experimentally observed high-amplitude oscillations of Hes1.

Recent studies have continued to explore complex dynamical behaviors in delayed systems across

various scientific domains. For example, fractional-order and stochastic models with state-dependent delays have been investigated to better understand controllability and long-term behavior in infinite-dimensional or neutral-type systems [19–22]. These works have introduced advanced mathematical tools such as the Mönch-type fixed point theorem, measure of noncompactness, and optimization strategies for trajectory tracking. Although these studies focus on engineering or control-theoretic applications, the methodologies they develop—particularly those involving non-instantaneous impulses, stochastic noise, and functional differential equations—highlight the growing interest in realistic modeling of biological and physical systems with delay. Such approaches could inspire future extensions of gene regulation models, especially in contexts where noise, spatial heterogeneity, or adaptive delay mechanisms are biologically relevant.

Given that transcription occurs in the nucleus and translation in the cytoplasm with mRNA diffusing to the cytoplasm and Hes1 protein diffusing back to the nucleus, Sturrock et al. [23] further extended previous models into a partial differential equation (PDE) framework. This PDE approach describes the spatio-temporal evolution of Hes1-mRNA concentrations more comprehensively. There is an ongoing effort to make Hes1 models more accurate, biologically realistic, and capable of capturing the sustained oscillatory behavior observed in experimental studies. Table 1 provides a summary of the key Hes1 models and their primary findings.

Notably, Sturrock et al. [23] were among the first to incorporate reaction-diffusion dynamics into Hes1-mRNA modeling to account for spatial effects. The model proposed in [23] used an indicator function in the cytoplasmic equation to approximate the timing of Hes1 protein production. This assumption, while useful numerically, introduces discontinuities that limit theoretical analysis, such as deriving analytic criteria for Hopf bifurcation. Our contribution is to develop a delayed reaction-diffusion model that overcomes this limitation by incorporating biologically meaningful transcriptional and translational delays instead of non-smooth approximations. We establish sufficient conditions for the existence of stable periodic oscillations using theoretical analysis, which accounts for both temporal delay and spatial diffusion. This allows us to derive a critical delay threshold at which Hopf bifurcation occurs, a task not addressed in prior spatial models. We clarifies the role of delay in producing sustained oscillations in a spatially extended framework and bridges the gap between temporal DDE models and spatial PDE systems. While our approach is motivated by the spatial compartmentalization used in [23], the models are structurally distinct, particularly in the use of no-flux boundaries and import/export terms rather than free diffusion between compartments. Through analytical and numerical approaches we validate the theoretical findings and demonstrate that our model produces biologically consistent oscillations in both space and time.

The remainder of this paper is organized as follows. In Section 2, we outline the modeling efforts and compare key models that study Hes1-mRNA interactions. We also discuss Monk's model in detail and analytically derive the critical value of τ at which the system exhibits stable periodic oscillations using linear stability analysis. In Section 3, we extend the previous reaction-diffusion model to a delayed reaction-diffusion framework, providing justifications for all the terms introduced. Additionally, we demonstrate that the previous model fails to produce stable periodic oscillations. In Section 4, we perform stability and oscillation analyses to derive conditions under which the system undergoes Hopf bifurcation. In Section 5, we present numerical examples to verify the theoretical results from Sections 2 and 4. Finally, Section 6 offers a discussion of the findings and their implications.

Table 1. Notable models of Hes1 dynamics with their biological relevance key findings.

Authors (Year published)	Model	Main result
Y. Zhang, J. Cao (2024)	DDE	Proposed a delay model to explore the dynamics of neural progenitor fate decisions [24].
A. Giri, S. Kar (2023)	SMA	Modeling to understand how cell-to-cell communication via the Notch signaling pathway leads to synchronization of Hes1 gene expression in noisy environments [25].
A. Rowntree, N. Sabherwal (2022)	ODE	The model was developed to simulate the interactions between Hes1 gene expression and the cell cycle [26].
S. Nath Singh, Md. Z. Malik (2020)	ODE	Modeling study of the Hes1-Notch-miR-9 regulatory network, demonstrating how Notch-induced changes drive different states of Hes1 and miR-9 dynamics [27].
T. Iwasaki, R. Takiguchi (2019)	ODE	Numerical simulations and mathematical modeling to study the behavior of neural differentiation [28].
M. Boareto, D. Iber (2017)	ODE[(1)]	Modeling to predict interactions between Notch signaling [29].
Sh. Li, Y. Liu (2016)	ODE	The ODE model includes the roles of microRNA, specifically miR-9, to understand how Hes1 oscillations are produced and controlled [30].
H. Wang, Y. Huang (2015)	ODE	A comprehensive mathematical model was proposed to simulate the dynamics of the Notch, Wnt, and FGF pathways in the segmentation clock [31].
M. Sturrock, A. Hellander (2014)	SMA	Extended a spatial stochastic model of the Hes1 GRN to include nuclear transport and dimerization of Hes1 monomers [32].
S. Li, Z. Liu (2014)	ODE	Aimed to understand the diverse expression patterns of Hes1 during the development of the central nervous system (CNS) [33].
A. Barton, A. J. Fendrik (2013)	ODE	Modified a previous gene network model for two cells coupled by the Delta-Notch pathway to analyze the effects of asymmetry in Notch degradation rates [34].
M. Sturrock, A. J. Terry (2012)	PDE	Extended PDE models to better capture the dynamics of Hes1 and p53–Mdm2 signaling pathways, including nuclear membrane and active transport mechanisms [35].
M. A. Tabatabai, W. M. Eby (2012)	ODE	Introduced a new model to capture and analyze various types of oscillatory behaviors observed in biomedical data [36].
M. Sturrock, A. J. Terry (2011)	PDE	Extended an ODE model to a PDE framework to describe the spatio-temporal evolution of Hes1 mRNA and Hes1 protein concentrations [23].
M. Bani-Yaghoub, D Amundson (2010)	PDE	Periodic dynamics of notch activity in a model of interacting signaling pathways [37].
H. Momiji, N. A. M. Monk (2008)	DDE	Extended DDE model to include nucleo-cytoplasmic transport, Hes1 monomers, and dimers, better capturing the high amplitude of Hes1 oscillations [18].
K. Rateitschak, O. Wolkenhauer (2007)	DDE	Modified a DDE model to account for distributed time delay, improving the model's accuracy [17].
S. Bernard, B. Cajavec (2006)	DDE	Addressed the overshooting problem in Hes1 expression by modifying the DDE to account for the Gro protein, aligning with experimental data [16].
M. H. Jensen, K. Sneppen, G. Tiana (2003)	DDE	The Hes1 network was modeled using a time delay approach, highlighting the critical role of degradation times in determining oscillatory behavior [13].
H. Hirata, S. Yoshiura (2002)	ODE[(1)]	Proposed an ODE model of Hes1 protein, hes1 mRNA, and a Hes1-interacting factor to achieve a oscillatory solutions [12].

Note: Abbreviations: PDE: Partial Differential Equations; DDE: Delayed Differential Equations; SMA: Stochastic Modeling Approach. [(1)] The modeling and simulations were accompanied by experimental data collected for this study.

2. Modeling efforts and preliminary results

In this section, we present the modeling efforts and discuss the significance of Monk's model [14]. The approach is foundational to understand the Hes1-mRNA interaction, as it introduced a simplified yet effective framework. The model was developed shortly after Hirata's pivotal experimental study where Monk replaced the system of three ordinary differential equations (ODE) with two delay differential equations (DDE), providing a more efficient representation that still matched experimental observations. This advancement has made Monk's formulation a cornerstone in modeling Hes1 dynamics, even when extended to more complex interactions involving other genes.

2.1. The Hes1-mRNA models

Table 2. Descriptions of models of mRNA (M) and Hes1 (H). For some models, the concentrations in the cytoplasm and the nucleus are denoted by subscripts c and n, respectively.

Hes1 model	Model description, justification and results
$M' = \alpha_m G[H(t-\tau)] - \mu_m M$ $H' = \alpha_p M - \mu_p H$	Monk's model [14] describes the rate of change of mRNA (M) and Hes1 protein (H) by incorporating transcriptional delay, production, and degradation. Simulation results show sustained oscillations when the delay exceeds a critical value and the Hill coefficient is sufficiently high ($n > 4$). No analytical results are provided.
$M' = \alpha G[H(t-\tau)] - \frac{M}{\tau_{rna}}$ $H' = \beta M - \frac{H}{\tau_{hes1}}$	Jensen's model [13] incorporates Hill functions and a discrete time delay to describe transcriptional and translational regulation in Hes1 and mRNA dynamics. The study uses numerical simulations to show that the delay can induce sustained or damped oscillations, depending on its magnitude.
$M' = b \cdot G[H_{CDF}(t-\tau)] - a \cdot M$ $H' = b \cdot M - a \cdot H$	Rateitschak and Wolkenhauer [17] extend Monk's model by introducing a distributed delay via a Gamma kernel. Using linear stability analysis, they derive a characteristic equation distinct from the discrete case and identify two Hopf bifurcation points, leading to a stability–oscillation–stability transition over a finite delay range.
$H'(t) = f_0 G[H(t-\tau)] - \alpha H(t)$ $GroH'(t) = g_0 \phi[H(t)] - \sigma GroH(t)$	Bernard et al. [16] perform linear stability analysis on Jensen's model to derive critical values of the Hill coefficient and delay that lead to Hopf bifurcation. In the extended model with Gro/TLE1, they show that oscillations depend on the product of two Hill coefficients, and derive corresponding critical thresholds.
$H' = -aHZ + bM - cH$ $M' = -dM + eG[H(t)]$ $Z' = -aHZ + fG[H(t)] - gZ$	Hirata's model [12] introduces an additional variable Z, representing a chemical entity interacting with Hes1 to achieve oscillatory behavior observed in experimental data.
$[M_n]' = D_{M_n}\nabla^2[M_n] + \alpha_m G[H_n(t)] - \mu_m[M_n]$ $[M_c]' = D_{M_c}\nabla^2[M_c] - \mu_m[M_c]$ $[H_c]' = D_{H_c}\nabla^2[H_c] + \alpha_H[M_c] - \mu_H[H_c]$ $[H_n]' = D_{H_n}\nabla^2[H_n] - \mu_H[H_n]$	Sturrock et al. [23] extended the Hes1 model by incorporating reaction-diffusion term and a characteristic function to localize Hes1 protein production. Using numerical simulations, they identified parameter regimes and spatial regions that support sustained oscillations, and showed that protein synthesis must occur at an optimal distance from the nucleus to maintain oscillatory behavior.
$M' = v_1 G[H(t)] - v_2 \phi[M(t)] - dMM_{miR-9}$ $H_c' = v_3 M - v_4 \phi[H_c(t)] - v_5 H_c$ $H_n' = v_5 H_c - v_6 \phi[H_n(t)]$ $B' = v_7 + v_8 \frac{B^2}{1+K_7 B^2 + K_8 H_n^2} - v_9 B$	Li et al. [33] extend a Hes1 model by adding BM88 dynamics with self-activation and Hes1 repression. They show BM88 exhibits bistability via a saddle-node bifurcation under constant Hes1, and a Hopf bifurcation arises in Hes1 dynamics as the nuclear transport rate (v_5) varies. Oscillatory Hes1 input enables more robust switching of BM88, highlighting its role in fate regulation.

The differential equations describing the dynamics are given by:

$$M' = \alpha_m G(P(t-\tau)) - \mu_m M(t) \tag{2.1}$$

$$P' = \alpha_p M(t) - \mu_p P(t), \tag{2.2}$$

where μ_m and μ_p denote the degradation rates of mRNA and protein, respectively. The parameter α_m signifies the basal rate of transcript initiation in the absence of Hes1 protein, while α_p represents the protein production rate, assuming an mRNA degradation rate of 0.03/min. The delayed feedback in the system is modeled by the Hill function $G(P(t-\tau))$, which is described by the equation:

$$G(P(t-\tau)) = \frac{1}{1 + \left(\frac{P(t-\tau)}{P_0}\right)^n} \tag{2.3}$$

where P_0 is the half-maximal effective concentration, and n is the Hill coefficient, reflecting the cooperativity of the inhibition [15].

To examine how subsequent extensions and modifications have built upon this foundational modeling framework and to address additional biological complexities, Table 2 provides a concise comparison of these key Hes1-mRNA models. By organizing these models side by side, the table highlights the progression from basic formulations to more advanced approaches that incorporate elements such as distributed delays, spatial dynamics, and additional regulatory components. In addition to the models presented in Table 2, there are several other sophisticated models that include Hes1 protein and mRNA. For instance, Singh et al. [27] developed an ODE model to study the Hes1-Notch-miR-9 regulatory network, demonstrating how Notch-induced changes drive different states of Hes1 and miR-9 dynamics. Furthermore, Hong-yan Wang [31] developed a model containing 33 differential equations to simulate the dynamics of the Notch, Wnt, and FGF pathways in the segmentation clock. This comprehensive model included three main genes: Notch1, Hes1, and RBP-jk. Moreover, Amitava Giri and colleagues [25] developed a model to understand how cell-to-cell communication via signaling pathways, specifically the Notch signaling pathway, leads to population-level synchronization of Hes1 gene expression in noisy cellular environments. Other models of Notch signaling pathway include those proposed in [37–39], which explore explore Turing-type instabilities and axon formation.

2.2. Periodic solutions of Monk's model

We rescale system (2.1) and (2.2) as in [14]. Specifically, we set

$$m = \frac{M}{\alpha_m}, \quad p = \frac{P}{\alpha_m \alpha_p}, \quad p_0 = \frac{P_0}{\alpha_m \alpha_p}.$$

This rescaling gives the following system with only two parameters:

$$m' = G(p(t-\tau)) - \mu_m m(t), \tag{2.4}$$

$$p' = m(t) - \mu_p p(t). \tag{2.5}$$

Suppose (m^*, p^*) is the equilibrium solution of the system. We aim to linearize the system around the point (m^*, p^*). The linearization process yields the following matrix representation:

$$\begin{bmatrix} m' \\ p' \end{bmatrix} = \begin{bmatrix} -\mu_m & 0 \\ 1 & -\mu_p \end{bmatrix} \begin{bmatrix} m - m^* \\ p - p^* \end{bmatrix} + \begin{bmatrix} 0 & G'(p^*) \\ 0 & 0 \end{bmatrix} \begin{bmatrix} m - m^* \\ p(t-\tau) - p^* \end{bmatrix}. \tag{2.6}$$

Now, the characteristic equation is formulated as a quadratic delay equation:

$$\lambda^2 + (\mu_m + \mu_p)\lambda + \mu_m \mu_p - G'(P^*)e^{-\lambda\tau} = 0. \tag{2.7}$$

The solution of (2.7) will be expressed using the Lambert W function [40–42]. Namely, suppose $\lambda = p + iq$ is a root of the characteristic equation, then we derive:

$$p^2 - q^2 + ap + b = c\exp(-p\tau)cos(q\tau) \tag{2.8}$$

$$2pq + aq = -c\exp(-p\tau)sin(q\tau) \tag{2.9}$$

where $a = \mu_m + \mu_p$, $b = \mu_m \mu_p$, and $c = G'(P^*)$.

If there exists a root of the characteristic equation with a zero or positive real part, then the solution of the linearized system is not asymptotically stable [43]. Suppose the characteristic equation has a pair of purely imaginary roots, say $\pm i\sigma_0$. We let $p = 0$ and $q = \sigma_0$, then we get

$$-\sigma_0^2 + b + c\cos(\sigma_0\tau) = 0 \tag{2.10}$$

$$a\sigma_0 + c\sin(\sigma_0\tau) = 0 \tag{2.11}$$

These two equations determine the two unknowns σ_0 and τ_0 for the characteristic equation to have two purely imaginary roots. The values are given by

$$\sigma_0 = \pm\frac{\sqrt{-2b \pm \sqrt{4b^2 - 4(b^2 - c^2)}}}{2} \tag{2.12}$$

and

$$\tau_0 = \frac{\arcsin\left(\frac{a\sigma_0}{c}\right)}{\sigma_0}. \tag{2.13}$$

When τ approaches τ_0 from below ($\tau < \tau_0$), all roots of the characteristic equation have negative real parts. However, as τ crosses τ_0 from below to above ($\tau > \tau_0$), two roots gain positive real parts.

At $\tau = \tau_0$, the characteristic equation exhibits two purely imaginary roots, $\pm i\sigma_0$. Consequently, similar to [43], the linear homogeneous system admits a pair of linearly independent delay-induced periodic solutions:

$$\phi_1(t) = \sin(\sigma_0 t) \tag{2.14}$$

$$\phi_2(t) = \cos(\sigma_0 t). \tag{2.15}$$

In the next section, we introduce our extended reaction-diffusion model of Hes1-mRNA interactions in the nucleus and cytoplasm.

3. Proposed Hes1-mRNA model

3.1. Sturrock model

Marc Sturrock [23] introduced a PDE-based extension of Monk's model that describes the dynamics of Hes1-mRNA in the nucleus and cytoplasm. This extended model incorporates both spatial and temporal dynamics, explicitly accounting for spatial interactions within the cell. The nucleus and cytoplasm are treated as two distinct spatial compartments, separated by the nuclear membrane, with the cytoplasm enclosed by the outer cell membrane. This approach provides a more comprehensive representation of intracellular processes by capturing the influence of spatial distributions.

The system of reaction-diffusion equations describing this model is as follows:

$$[M_n(x,t)]' = D_1\nabla^2[M_n(x,t)] + \alpha_m G[H_n(x,t-)] - \mu_m[M_n(x,t)], \tag{3.1}$$

$$[M_c(x,t)]' = D_2\nabla^2[M_c(x,t)] - \mu_m[M_c(x,t)], \tag{3.2}$$

$$[H_c(x,t)]' = D_3\nabla^2[H_c(x,t)] + \alpha_H[M_c(x,t)] - \mu_H[H_c(x,t)], \tag{3.3}$$

$$[H_n(x,t)]' = D_4\nabla^2[H_n(x,t)] - \mu_H[H_n(x,t)]. \tag{3.4}$$

In this system of equations, M_n represents the mRNA concentration in the nucleus, and M_c denotes the mRNA concentration in the cytoplasm. Likewise, H_n is the concentration of Hes1 protein in the nucleus, and H_c is the Hes1 protein concentration in the cytoplasm. The diffusion coefficients D_1, D_2, D_3, and D_4 correspond to the diffusion of mRNA in the nucleus, mRNA in the cytoplasm, Hes1 protein in the cytoplasm, and Hes1 protein in the nucleus, respectively. The parameters μ_m and μ_H are the degradation rates for mRNA and Hes1 protein, respectively. The production rates are given by α_m for mRNA and α_H for Hes1 protein.

In system (3.1)–(3.4), the author accounts for the delay by incorporating a function that localizes protein production. This approach assumes that the delay arises solely from spatial diffusion. However, in biological systems, delays are influenced by a combination of processes, including transcription, translation, nuclear transport, and other regulatory mechanisms. Monk's model [14] demonstrated that the observed oscillatory expression is most likely driven by transcriptional and translational delay. Therefore, incorporating a transcriptional delay is crucial for accurately modeling the system. In contrast to relying solely on spatially localized production, our model incorporates a biologically motivated delay term to reflect the combined effects of transcriptional, translational, and spatial dynamics. This allows us to analyze the influence of both spatial diffusion and time delays, and to derive analytical conditions under which stable periodic oscillations can emerge. Furthermore, we analytically demonstrate that the original model without the indicator function fails to produce stable periodic oscillations, reinforcing the importance of explicitly incorporating biologically realistic delays.

Theorem 1. ***[Global Stability]*** *Model (3.1)–(3.4) has a unique globally asymptotically stable equilibrium solution given by*

$$(M_n^*, M_c^*, H_c^*, H_n^*) = \left(\frac{\alpha_m}{\mu_m}, 0, 0, 0\right).$$

Proof. At equilibrium, we set $[M_n]' = [M_c]' = [H_c]' = [H_n]' = 0$, reducing the system to:

$$\begin{aligned} 0 &= \alpha_m G(H_n) - \mu_m[M_n], \\ 0 &= -\mu_m[M_c], \\ 0 &= \alpha_H[M_c] - \mu_H[H_c], \\ 0 &= -\mu_H[H_n]. \end{aligned}$$

The equilibrium point is:

$$(M_n^*, M_c^*, H_c^*, H_n^*) = \left(\frac{\alpha_m}{\mu_m}, 0, 0, 0\right).$$

Using linear stability analysis, the eigenvalues of the system are:

$$\lambda_1 = -(\mu_m + D_1k^2), \quad \lambda_2 = -(\mu_m + D_2k^2), \quad \lambda_3 = -(\mu_H + D_3k^2), \quad \lambda_4 = -(\mu_H + D_4k^2),$$

where k is the wavenumber. Since all diffusion coefficients are nonnegative, $\mu_m > 0$ and $\mu_H > 0$, all eigenvalues are negative, and the equilibrium point is locally stable. Therefore, nearby solutions of the system asymptotically converge to $(M_n^*, M_c^*, H_c^*, H_n^*)$.

It can be easily shown that the stability is global. From Eq (3.4), we get that the value of H_N should exponentially decay and converge to 0. Similarly, from Eq (3.2), we get that the value of M_C must go to 0 as t goes to infinity. Since M_C converges to 0 from Eq (3.3), we get that H_C will also converge to 0. From Eq (2.3), we get that $G(0) = 1$ and therefore Eq (3.3) implies that M_n must converge to $\frac{\alpha_m}{\mu_m}$ as t goes to infinity.

Remark 1. ***[nonresistance of the stable periodic solutions]*** *Theorem 1 implies that all solutions of model (3.1)–(3.4) with nonnegative initial conditions must converge to the equilibrium $(M_n^*, M_c^*, H_c^*, H_n^*)$. Hence, the model cannot exhibit stable periodic solutions.*

Remark 2. *To address the absence of periodic solutions, Sturrock et al. [23] introduced a step function into Eq (3.3), enabling the production of the Hes1 protein beyond a specific spatial threshold. This modification facilitates the emergence of sustained oscillatory behavior in the system.*

3.2. Proposed model

Our model is motivated by the compartmental reaction-diffusion framework developed in [23]. Specifically, to allow the diffusion-reaction model to exhibit a stable periodic solution, we first extend model (3.1)–(3.4) by incorporating a delay term to account for transcription and translation. As in Monk's model, the delay τ represents the combined effect of transcriptional and translational time delays. However, it can be shown that incorporating a delay term alone is insufficient for the model to exhibit a stable periodic solution. To address this, we further modified the model to include export and import terms, as described in [18]. This leads to the following extended model:

$$M_n' = D_1\nabla^2 M_n + \alpha_m G\left(H_n(t-\tau)\right) - \mu_m M_n, \tag{3.5}$$

$$M_c' = D_2\nabla^2 M_c - \mu_m M_c + \gamma_1 M_n, \tag{3.6}$$

$$H_c' = D_3\nabla^2 H_c + \alpha_H M_c - \mu_H H_c, \tag{3.7}$$

$$H_n' = D_4\nabla^2 H_n - \mu_H H_n + \gamma_2 H_c. \tag{3.8}$$

For the purpose of simulations, we considered a one-dimensional spatial domain of length $L = 10$ micrometers, representing the cell diameter. Hence, our model assumes the spatial domain includes the nucleus and cytoplasm. The dynamics of the nucleus and cytoplasm are captured by separate equations for each region. We applied zero-flux Neumann boundary conditions:

$$\frac{\partial M_n}{\partial x} = \frac{\partial M_c}{\partial x} = \frac{\partial H_c}{\partial x} = \frac{\partial H_n}{\partial x} = 0 \quad \text{at} \quad x = 0 \text{ and } x = L.$$

These conditions ensure zero flux, meaning no molecules are lost through the cell boundaries, reflecting the closed nature of the cellular environment.

The delay term τ represents the time required for gene expression to exert negative feedback. Specifically, it accounts for the time it takes for the Hes1 gene to be transcribed into mRNA in the nucleus, and for that mRNA to be translated into Hes1 protein in the cytoplasm. This includes transcriptional initiation, elongation, mRNA processing, and cytoplasmic translation. By distinguishing between these mechanisms, the model allows us to analyze how transcriptional/translational timing and spatial diffusion jointly influence the emergence of stable oscillations.

Here, γ_1 represents the rate of import of mRNA to the cytoplasm, and γ_2 denotes the rate of import of the Hes1 protein to the nucleus. The parameter μ_m accounts for the combined effects of the degradation rate and the export rate of mRNA, while μ_H represents the degradation rate plus the export rate of Hes1 protein. In Table 3, we summarize the parameters and variables used in the extended model (3.5)–(3.8). All other variables and parameters remain the same as in the previous model.

Table 3. Description of parameters, symbols, variables, and units in model (3.5)–(3.8).

Symbol	Description	Unit
M_n	mRNA concentration in the nucleus	nM
M_c	mRNA concentration in the cytoplasm	nM
H_c	Hes1 protein concentration in the cytoplasm	nM
H_n	Hes1 protein concentration in the nucleus	nM
α_m	Production rate of mRNA	nM/h
α_H	Production rate of Hes1 protein	nM/h
μ_m	Degradation rate and export rate of mRNA	1/h
μ_H	Degradation rate and export rate of Hes1 protein	1/h
γ_1	Rate of mRNA import to the cytoplasm	1/h
γ_2	Rate of Hes1 protein import to the nucleus	1/h
τ	Delay term for transcription and translation	h
∇^2	Laplacian operator accounting for diffusion	–
$G[H_n(t-\tau)]$	Hill function modeling delayed feedback in transcription	–
D_1, D_2, D_3, D_4	Diffusion coefficients for mRNA and Hes1 protein in the nucleus and cytoplasm	μm²/h

Note: nM = 10^{-9} moles per liter ($nmol/L$), h = hour, and $\mu m^2/h$ =square micrometers per hour.

4. Analysis of the extended model

4.1. Stability and oscillation

Let $(M_n^*, M_c^*, H_c^*, H_n^*)$ be the positive equilibrium solution of system (3.5)–(3.8). We get that

$$\alpha_m G(H_n^*) - \mu_m(M_n^*) = 0 \tag{4.1}$$

$$-\mu_m(M_c^*) + \gamma_1 M_n^* = 0 \tag{4.2}$$

$$\alpha_H M_c^* - \mu_H H_c^* = 0 \tag{4.3}$$

$$-\mu_H H_n^* + \gamma_2 H_c^* = 0 \tag{4.4}$$

Let the deviations from equilibrium be defined as follows:

$$V_1(t,x) = M_n - M_n^*, \tag{4.5}$$

$$V_2(t,x) = M_c - M_c^*, \tag{4.6}$$

$$V_3(t,x) = H_c - H_c^*, \tag{4.7}$$

$$V_4(t,x) = H_n - H_n^*. \tag{4.8}$$

The linearized system around the equilibrium is given by:

$$\frac{\partial V_1(t,x)}{\partial t} = D_1\nabla^2 V_1(t,x) + \alpha_m G'(H_n^*)\cdot V_4(t-\tau,x) - \mu_m V_1(t,x), \tag{4.9}$$

$$\frac{\partial V_2(t,x)}{\partial t} = D_2\nabla^2 V_2(t,x) - \mu_m V_2(t,x) + \gamma_1 V_1(t,x), \tag{4.10}$$

$$\frac{\partial V_3(t,x)}{\partial t} = D_3\nabla^2 V_3(t,x) + \alpha_H V_2(t,x) - \mu_H V_3(t,x), \tag{4.11}$$

$$\frac{\partial V_4(t,x)}{\partial t} = D_4\nabla^2 V_4(t,x) - \mu_H V_4(t,x) + \gamma_2 V_3(t,x). \tag{4.12}$$

Let:

$$V = \begin{pmatrix} V_1 \\ V_2 \\ V_3 \\ V_4 \end{pmatrix}$$

and

$$D = \mathrm{diag}(D_1, D_2, D_3, D_4).$$

For $\Phi = (\phi_1, \phi_2, \phi_3, \phi_4)^T \in \zeta = C(-\tau, X)$, we can write the system in abstract differential form as follows:

$$\dot{V}(t) = D\nabla^2 V(t) + L(V), \tag{4.13}$$

where the linear operator $L : \xi \to X$ is given by:

$$L(\Phi) = B_0\Phi(0) + B_1\Phi(-\tau).$$

Here, the matrix B_0 is defined as:

$$B_0 = \begin{pmatrix} -\mu_m & 0 & 0 & 0 \\ \gamma_1 & -\mu_m & 0 & 0 \\ 0 & \alpha_H & -\mu_H & 0 \\ 0 & 0 & \gamma_2 & -\mu_H \end{pmatrix}.$$

The matrix B_1 is given by:

$$B_1 = \begin{pmatrix} 0 & 0 & 0 & \alpha_m G'(H_n^*) \\ 0 & 0 & 0 & 0 \\ 0 & 0 & 0 & 0 \\ 0 & 0 & 0 & 0 \end{pmatrix}.$$

The characteristic polynomial of Eq (4.13) is as follows:

$$\lambda Y - D\nabla^2 Y - L(e^{\lambda\tau}Y) = 0, \quad Y \in \mathrm{dom}(\nabla^2)\backslash\{0\}.$$

Let $-k^2$ $(k = 0, 1, 2, \ldots)$ be the eigenvalue of ∇^2 on the domain X with the corresponding eigenvectors:

$$\beta_k^1 = \begin{pmatrix} v_k \\ 0 \\ 0 \\ 0 \end{pmatrix}, \quad \beta_k^2 = \begin{pmatrix} 0 \\ v_k \\ 0 \\ 0 \end{pmatrix}, \quad \beta_k^3 = \begin{pmatrix} 0 \\ 0 \\ v_k \\ 0 \end{pmatrix}, \quad \beta_k^4 = \begin{pmatrix} 0 \\ 0 \\ 0 \\ v_k \end{pmatrix},$$

where $v_k = \cos(kx)$. Then, we can expand the solution in the form of a Fourier series on the phase space X. By following the same steps as in [44], we can get the following determinant:

$$\det\begin{pmatrix} \lambda+\mu_m+d_1k^2 & 0 & 0 & -\alpha_m G'(H_n^*)e^{-\lambda\tau} \\ -\gamma_1 & \lambda+\mu_m+d_2k^2 & 0 & 0 \\ 0 & -\alpha_H & \lambda+\mu_H+d_3k^2 & 0 \\ 0 & 0 & -\gamma_2 & \lambda+\mu_H+d_4k^2 \end{pmatrix}.$$

By evaluating the determinant, we get the characteristic equation:

$$(\lambda+\mu_m+d_1k^2)(\lambda+\mu_m+d_2k^2)(\lambda+\mu_H+d_3k^2)(\lambda+\mu_H+d_4k^2) - \gamma_1\gamma_2\alpha_H\alpha_m G'(H_n^*)e^{-\lambda\tau} = 0. \quad (4.14)$$

Equation (4.14) can be rewritten as:

$$\lambda^4 + A_1\lambda^3 + A_2\lambda^2 + A_3\lambda + A_4 - ge^{-\tau\lambda} = 0, \quad (4.15)$$

where:

$$A_1 = 2\mu_m + d_1k^2 + d_2k^2 + d_3k^2 + d_4k^2 + 2\mu_H,$$

$$A_2 = \mu_m^2 + \mu_m d_1k^2 + \mu_m d_2k^2 + 2\mu_m d_3k^2 + 2\mu_m d_4k^2 + 4\mu_m\mu_H + d_1d_2k^4$$
$$+d_1d_3k^4 + d_1d_4k^4 + 2\mu_H d_1k^2 + d_2d_3k^4 + d_2d_4k^4 + 2\mu_H d_2k^2 + d_3d_4k^4 + \mu_H d_3k^2 + \mu_H d_4k^2 + \mu_H^2.$$

$$A_3 = 2\mu_H^2\mu_m + 2\mu_H\mu_m d_4k^2 + 2\mu_H\mu_m d_3k^2 + 2\mu_m d_3d_4k^4 + \mu_H^2 d_2k^2 + \mu_H d_2d_4k^4$$
$$+\mu_H d_2d_3k^4 + d_2d_3d_4k^6 + 2\mu_m^2\mu_H + \mu_m^2 d_4k^2 + \mu_m^2 d_3k^2 + 2\mu_m\mu_H d_2k^2 + \mu_m d_2d_4k^4 + \mu_m d_2d_3k^4$$
$$+\mu_H^2 d_1k^2 + \mu_H d_1d_4k^4 + \mu_H d_1d_3k^4 + d_1d_3d_4k^6 + 2\mu_m\mu_H d_1k^2 + \mu_m d_1d_4k^4 + \mu_m d_1d_3k^4$$
$$+\mu_H d_1d_2k^4 + d_1d_2d_4k^6 + \mu_H d_1d_2k^4 + \mu_H d_1d_2d_3k^6$$

$$A_4 = \mu_m^2\mu_H^2 + \mu_m^2\mu_H d_4k^2 + \mu_m^2\mu_H d_3k^2 + \mu_m^2 d_3d_4k^4 + \mu_m\mu_H^2 d_2k^2 + \mu_m\mu_H d_2d_4k^4$$
$$+\mu_m\mu_H d_2d_3k^4 + \mu_m d_2d_3d_4k^6 + \mu_m\mu_H^2 d_1k^2 + \mu_H\mu_m d_1d_4k^4 + \mu_m\mu_H d_1d_3k^4 + \mu_m d_1d_3d_4k^6$$
$$+\mu_H^2 d_1d_2k^4 + \mu_H d_1d_2d_4k^6 + \mu_H d_1d_2d_3k^6 + d_1d_2d_3d_4k^8$$

Finally, the term g is given by:

$$g = \gamma_1\gamma_2\alpha_H\alpha_m G'(H_n^*).$$

Clearly, $A_1 > 0$ and $\lambda = 0$ is not a root of Eq (4.15) for all values of k. By the Routh-Hurwitz criterion, we have the following lemma.

Lemma 1. *If $\tau = 0$ and the conditions:*

(1) $A_1A_2 > A_3$
(2) $A_3 > \frac{A_1^2A_4 + A_1^2g}{A_1A_2 - A_3}$,
(3) $A_4 > g$,

Then all roots of Eq (4.15) have negative real parts.

Proof. By the *Routh-Hurwitz criterion* for a polynomial of degree 4, the system is stable if and only if all leading principal minors of the Routh array are positive. By letting $\tau = 0$ in the characteristic equation (4.15), we get

$$P(\lambda) = \lambda^4 + A_1\lambda^3 + A_2\lambda^2 + A_3\lambda + (A_4 - g). \tag{4.16}$$

Then, the Routh array is constructed as follows:

$$\begin{array}{c|cc} \lambda^4 & 1 & A_2 \quad A_4 - g \\ \lambda^3 & A_1 & A_3 \quad 0 \\ \lambda^2 & B_1 = \frac{A_1A_2 - A_3}{A_1} & B_2 = A_4 - g \\ \lambda^1 & C_1 = \frac{B_1A_3 - A_1B_2}{B_1} & \\ \lambda^0 & D_1 = B_2 & \end{array}$$

For stability, all entries in the first column of the Routh array must be positive. Since $A_i > 0$ for all $i = 1, \ldots, 4$, and by assuming the conditions given in the lemma hold, we conclude that:

$$B_1 > 0, \quad C_1 > 0, \quad D_1 > 0.$$

Thus, all Routh-Hurwitz conditions are satisfied, ensuring that all roots of Eq (4.15) have negative real parts.

Theorem 2. ***[nonexistence of stable periodic solution]*** *If γ_1 or γ_2 equals 0 with conditions (1) and (2) in Lemma 1 holding, then the system (3.5)–(3.8) cannot exhibit any stable periodic solution.*

Proof. Let $\gamma_1 = 0$. In this case, the characteristic equation (4.15) no longer contains the delay term. By Lemma 1, all roots of this reduced polynomial have negative real parts. Thus, the system remains stable near the positive equilibrium. A similar argument to the case $\gamma_2 = 0$.

4.2. Delay-induced periodic solution

The goal of this section is to find a critical value τ_0 where the positive equilibrium solution for model (3.5)–(3.8) loses its stability and a periodic solution bifurcates from it. Suppose $p + iq$ is a root of Eq (4.15). We get that

$$(p + iq)^4 + A_1(p + iq)^3 + A_2(p + iq)^2 + A_3(p + iq) + A_4 - ge^{-\tau(p+iq)} = 0. \tag{4.17}$$

By separating the real and the other imaginary parts, the following two equations are deduced. For the real part, we get:

$$p^4 - 6p^2q^2 + q^4 + A_1\left(p^3 - 3pq^2\right) + A_2\left(p^2 - q^2\right) + A_3p + A_4 - ge^{-\tau p}\cos(q\tau) = 0. \tag{4.18}$$

For the imaginary part, we get:

$$4pq(p^2 - q^2) + A_1\left(3p^2q - q^3\right) + 2A_2pq + A_3q + ge^{-\tau p}\sin(q\tau) = 0. \tag{4.19}$$

Assume we have a pure imaginary root $\pm i\sigma$. By Eqs (4.18) and (4.19), we have

$$\sigma^4 - A_2\sigma^2 + A_4 - g\cos(\sigma\tau) = 0, \tag{4.20}$$

$$-A_1\sigma^3 + A_3\sigma + g\sin(\sigma\tau) = 0. \tag{4.21}$$

From Eqs (4.20) and (4.21), we can derive an equation for σ as follows:

$$\sigma^8 + (-2A_2 + A_1^2)\sigma^6 + (A_2^2 - 2A_4 - 2A_1A_3)\sigma^4 + (2A_2A_4 + A_3^2)\sigma^2 + A_4^2 - g^2 = 0. \tag{4.22}$$

The following lemma establishes conditions for the existence of at most one positive real root for Eq (4.22).

Lemma 2. *If the conditions:*

(1) $A_1^2 > 2A_2$
(2) $A_2^2 > 2A_4 + 2A_1A_3$,
(3) $g^2 > A_4^2$,

Then there exists $K > 0$ *such that for* $0 \le k \le K$, *Equation (4.22) has at most one positive real root* σ_k.

Proof. This lemma is a direct implication of Descartes' [45].

From Lemma 2, we ensure that, under certain conditions, there exists a unique positive real value of σ. Using Eq (4.20), we can now derive the critical value of $\tau_k^{(j)}$ as follows:

$$\tau_k^{(j)} = \frac{1}{\sigma_k}\arccos\left(\frac{\sigma_k^4 - A_2\sigma_k^2 + A_4}{g}\right) + \frac{2j\pi}{\sigma_k}, \tag{4.23}$$

where $0 \le k \le K$, and $\tau_0^j \le \tau_1^j \le \tau_2^j \le \cdots \le \tau_K^j$, for $j = 0, 1, 2, \ldots$.

Let $\lambda(\tau) = \nu(\tau) + \sigma(\tau)i$ be a root of Eq (4.15) such that $\nu(\tau_k^j) = 0$ and $\sigma(\tau_k^j) = \sigma_k$. Furthermore, let $\tau_0^0 = \min\{\tau_k^0\}$. The following corollary, taken from [46–48], is necessary for proving the next theorem.

Corollary 1. *Consider the exponential polynomial*

$$\begin{aligned} P(\lambda, e^{-\lambda\tau}, \ldots, e^{-\lambda\tau_m}) = {} & \lambda^n + p_1^{(0)}\lambda^{n-1} + \cdots + p_{n-1}^{(0)}\lambda + p_n^{(0)} \\ & + [p_1^{(1)}\lambda^{n-1} + \cdots + p_{n-1}^{(1)}\lambda + p_n^{(1)}]e^{-\lambda\tau} + \cdots \\ & + [p_1^{(m)}\lambda^{n-1} + \cdots + p_{n-1}^{(m)}\lambda + p_n^{(m)}]e^{-\lambda\tau_m}, \end{aligned}$$

where $\tau_i \ge 0\,(i = 1, 2, \ldots, m)$ *and* $p_j^{(i)}\,(j = 1, 2, \ldots, n)$ *are constants. As* $(\tau_1, \tau_2, \ldots, \tau_m)$ *vary, the sum of the order of the zeros of* $P(\lambda, e^{-\lambda\tau}, \ldots, e^{-\lambda\tau_m})$ *in the open right half-plane can change only if a zero appears on or crosses the imaginary axis.*

Proof. The proof is provided in Section 2 of [46].

Theorem 3. ***[Existence of periodic solution]*** *If conditions (1)–(3) in Lemma 1 are satisfied and*

$$Re\left(\frac{d\lambda}{d\tau}\right)_{\tau=\tau_0} > 0,$$

The positive equilibrium solution of model (3.5)–(3.8) is locally asymptotically stable when $\tau \in [0, \tau_0^0)$, *and loses its stability when* $\tau = \tau_0^0$. *Moreover, periodic solutions bifurcate from the positive equilibrium when* τ *crosses the critical value* τ_0.

Proof. Let $\tau = 0$. By Lemma 1, the equilibrium is locally asymptotically stable under conditions (1)–(3). By Corollary 1, the transition to oscillatory behavior occurs only when the eigenvalue has zero real part. Such an event occurs at $\tau = \tau_0^0$. By the transversality condition, it follows that the eigenvalues move from the stable region to the unstable region as τ crosses τ_0^0 (see for example [49]).

5. Numerical simulations

We numerically examined the main results obtained in Sections 2 and 4. We first explored the solution behaviors of the Hes1-mRNA model (2.1) and (2.2) as the delay parameter τ varied around its critical value. We used the same parameter values as in [14], as illustrated in Table 4.

Table 4. Parameter values and range of values for model (2.1) and (2.2) simulations.

Symbol	Description	Baseline value and range	Reference
μ_m	Rate of mRNA degradation	0.03 (0.026, 0.03)	[14]
μ_p	Rate of protein degradation	0.03 (0.027, 0.036)	[14]
τ	Time delay	18.5 (10, 20)	[14, 18]
P_0	Reference protein concentration	100 (10, 100)	[14, 18]
n	Hill coefficient	5 (2, 10)	[14, 18]

The value of $G'(P^*)$, which represents the linearized Hill function at equilibrium, was taken from [50] for consistency with the parameter values. Specifically, $G'(P^*) = 3.9089 \times 10^{-3}$. A different approach was employed to calculate the critical value τ_0, but the result matched the value reported in [50]. Substituting the parameter values into Eq (2.12), we obtained $\sigma_0 = 5.4854 \times 10^{-2}$. Using this result in Eq (2.13), the critical delay value was calculated as $\tau_0 = 18.2470$. Figure 1 illustrates the numerical simulations performed to observe how the system transitions between a stable equilibrium and periodic solutions for values of τ near the analytically derived threshold. The results are presented as time-series plots and phase plane trajectories. For $\tau = 18$, which is below the critical value, the time-series data in Figure 1(a),(b) demonstrate that the solution converges to the equilibrium point. The phase plane trajectory spirals inward, confirming stability. When τ is increased to 19, which is above the critical value, periodic oscillations emerge, as depicted in Figure 1(c),(d). The time-series data show sustained oscillations, and the phase plane trajectory forms a closed orbit, indicating the presence of a limit cycle.

Next, using PDE toolbox, we explored several simulations to verify the theoretical results presented in Section 4. For the numerical simulations of extended model (3.5)–(3.8), we considered a one-dimensional (1D) spatial domain of length $L = 10$, representing the cell diameter. The zero flux boundary condition ensures that no molecules are lost through the cell boundaries, reflecting the closed nature of the cellular environment. We employed the initial conditions $M_n(x, 0) = 3$, $M_c(x, 0) = 0$, $H_c(x, 0) = 100$, and $H_n(x, 0) = 0$. These homogeneous profiles were selected based on the work of Monk et al. [14], specifically using $M_n = 3$ and $H_c = 100$. Additional simulations conducted with alternative initial conditions yielded qualitatively similar results, suggesting that the model's solutions are robust with respect to the choice of initial conditions.

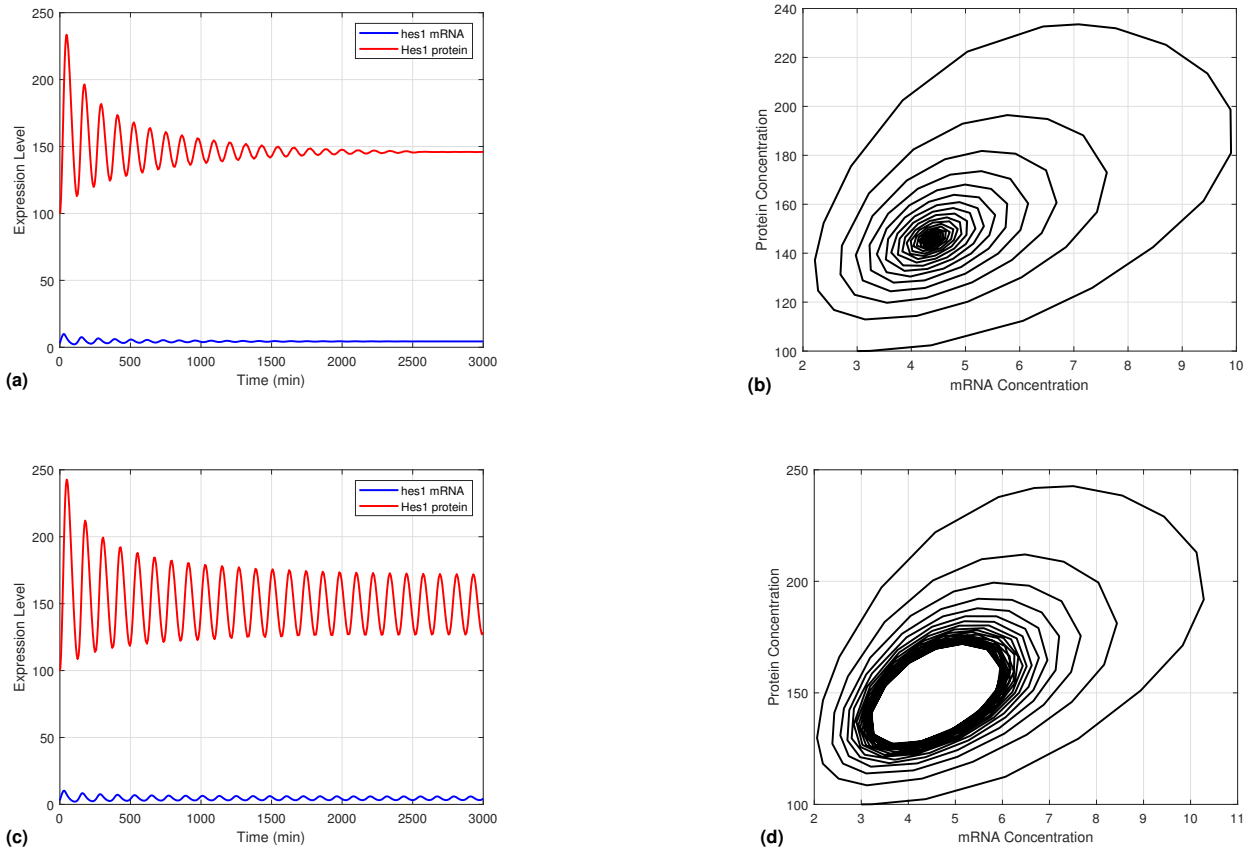

Figure 1. Dynamics of the Hes1 gene expression model (2.1) and (2.2) for delay τ near the critical value. (a) Conference to equilibrium solution for $\tau = 18$. (b) Corresponding phase plane for $\tau = 18$. (c) Periodic solutions for $\tau = 19$. (d) Corresponding limit cycle for $\tau = 19$. The parameter values are listed in Table 4.

Table 5. Parameter values for model (3.5)–(3.8) simulations.

Symbol	Description	Value	Reference
μ_m	Rate of mRNA degradation + export rate	0.03 + 0.05	[14]
μ_p	Rate of protein degradation + export rate	0.03 + 0.05	[14]
τ	Time delay	17, 18, 19	[14]
P_0	The repression threshold	80	[14]
n	Hill coefficient	5	[14]
γ_1	Rate of mRNA import to the cytoplasm	0.05	estimated
γ_2	Rate of Hes1 protein import to the nucleus	0.05	estimated
α_H	Hes1 protein production rate	2	[23]
α_m	mRNA production rate	1	[23]
D_i	Diffusion coefficient for $i = 1, 2, 3, 4$	7.5×10^{-4}	[23]

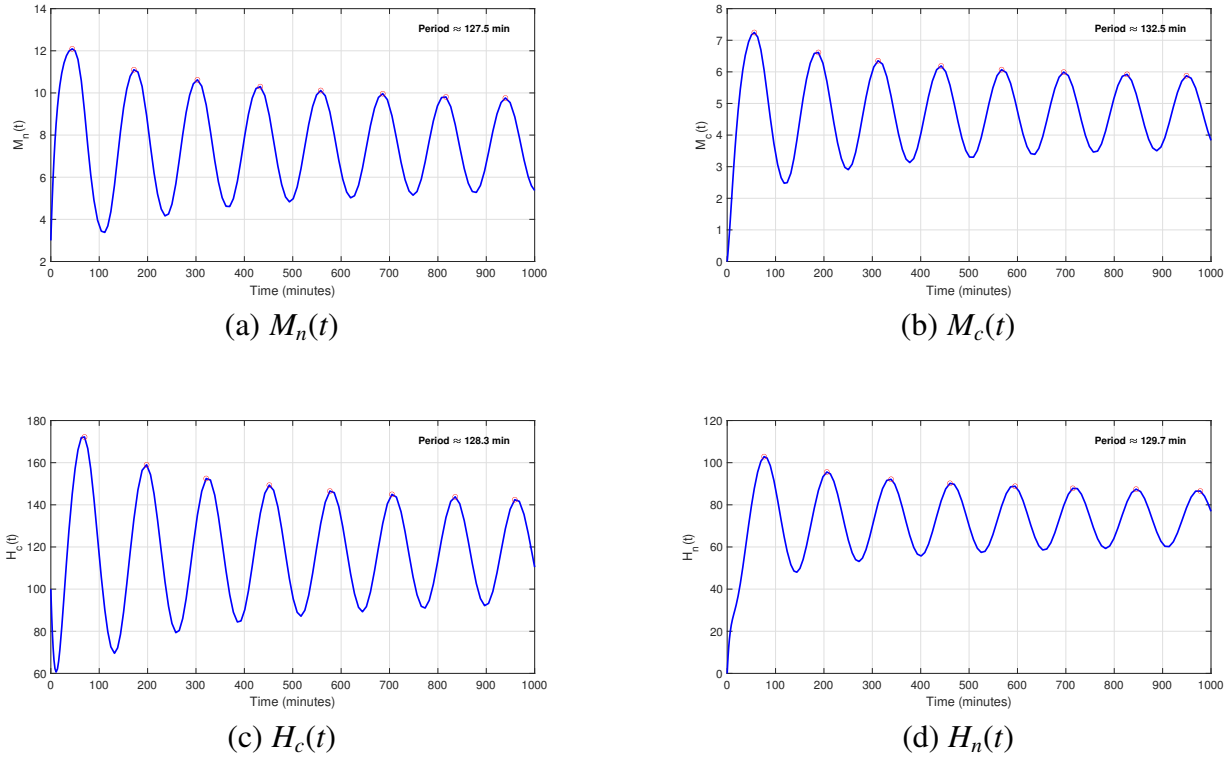

(a) $M_n(t)$ (b) $M_c(t)$

(c) $H_c(t)$ (d) $H_n(t)$

Figure 2. Time-series dynamics of the Hes1-mRNA expression model (3.5)–(3.8) simulated with a delay value of $\tau = 19$ near the Hopf bifurcation threshold. Each panel displays oscillatory behavior for one of the four key components of the system: (a) nuclear mRNA M_n, (b) cytoplasmic mRNA M_c, (c) cytoplasmic protein H_c, and (d) nuclear protein H_n. The oscillations are stable and periodic, with the estimated period annotated in each plot. Parameter values are listed in Table 5.

By calculating the system defined by Eqs (3.5)–(3.8), we identified a positive equilibrium solution: $H_n^* = 73.52$, $H_c^* = 117.70$, $M_n^* = 7.53$, and $M_c^* = 4.71$. Using the parameter values shown in Table 5, we compute the following coefficients: $A_1 = 0.32$, $A_2 = 0.0384$, $A_3 = 2.048 \times 10^{-3}$, $A_4 = 4.096 \times 10^{-5}$, and $g = -1.720 \times 10^{-4}$. We verified the conditions in Lemma 1 and confirmed that for $\tau \in (0, \tau_0^0)$, the system is locally asymptotically stable. Using Eq (4.22), we calculated $\sigma_0 = 0.0592955$, and from Eq (4.23), we determined $\tau_0^0 = 18.172$. Further simulations suggest that when $\tau = 17 < \tau_0^0$, the system converges to the equilibrium points. However, when $\tau = 19 > \tau_0^0$, the system exhibits stable periodic oscillations. The spatio-temporal evolution of Hes1 protein and mRNA in the nucleus and cytoplasm, both before and after the critical delay value, is illustrated in Figures 3 and 4. We used the parameter values provided in Table 5, as referenced in the cited literature. However, for the parameters γ_1 and γ_2, no experimental data are available. Therefore, we estimated their values based on experimental observations reported by [12], which indicate that the oscillation period should be approximately 2 hours. Using the parameter values from Table 5 and our estimation for γ_1 and γ_2, we obtained stable oscillations with a period slightly more than two hours (mean value of 129.25 minutes), as illustrated in Figure 2, which aligns well with the experimental observations [8].

To verify Theorem 2, we set $\gamma_1 = 0$ while keeping all other parameter values unchanged. Under

these conditions, the system converged to the equilibrium solution, and no oscillations were observed. These simulation results are in good agreement with Theorem 2.

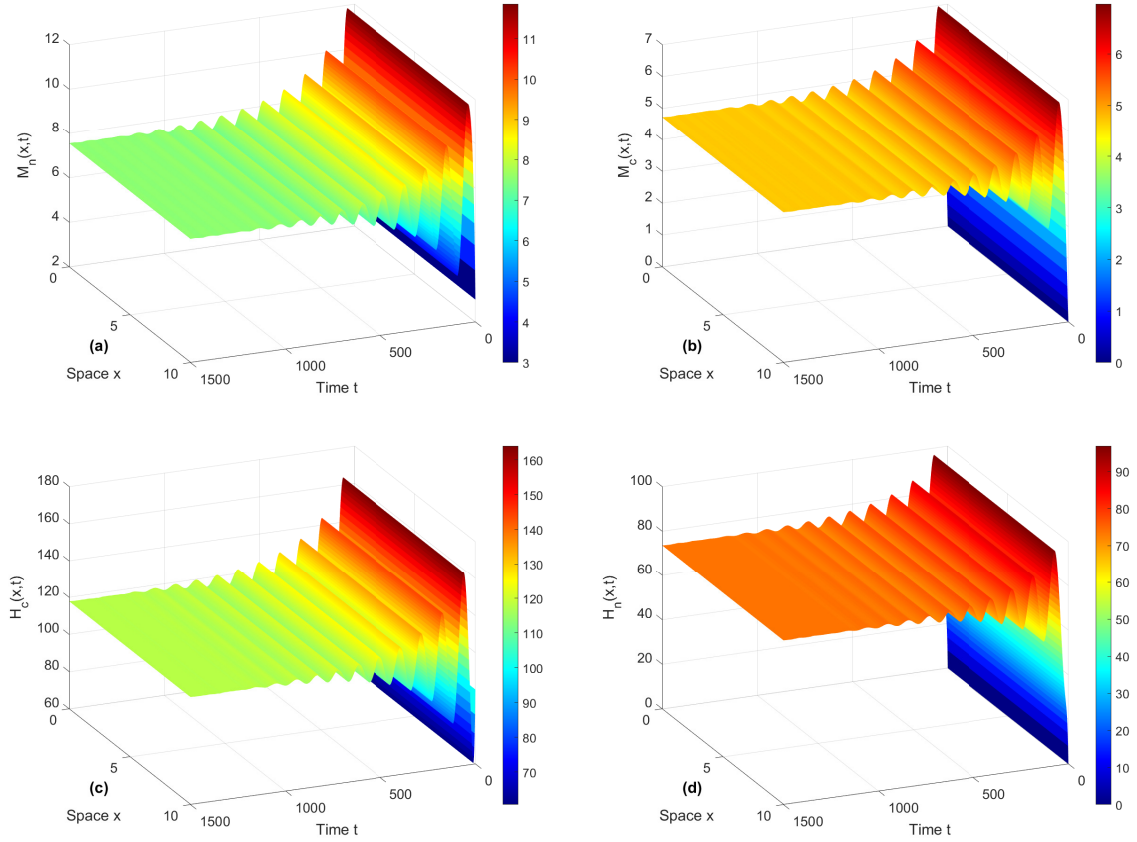

Figure 3. Spatio-temporal simulations for the Hes1 gene expression model (3.5)–(3.8) with delay $\tau = 17 < \tau_0^0$. (a) mRNA concentration in the nucleus, (b) mRNA concentration in the cytoplasm, (c) Hes1 protein concentration in the cytoplasm, and (d) Hes1 protein concentration in the nucleus.

6. Discussion

This study investigates the emergence of oscillatory behavior in the Hes1-mRNA system within a spatially extended framework, emphasizing how transcriptional/translational delays and diffusion interact to influence dynamic stability. We began by reviewing prominent models of the Hes1-mRNA system, summarizing their objectives and contributions in Table 1. Then, we proposed a delayed reaction-diffusion model of Hes1-mRNA interactions that incorporates transcriptional and translational delays, along with spatial diffusion within compartments and biologically motivated import-export terms, to explore the emergence of stable oscillations in a spatially extended system. The model by Sturrock et al. [23] used an indicator function to induce oscillatory behavior through spatial positioning, but it did not incorporate explicit transcriptional and translational delays. In contrast, our model includes

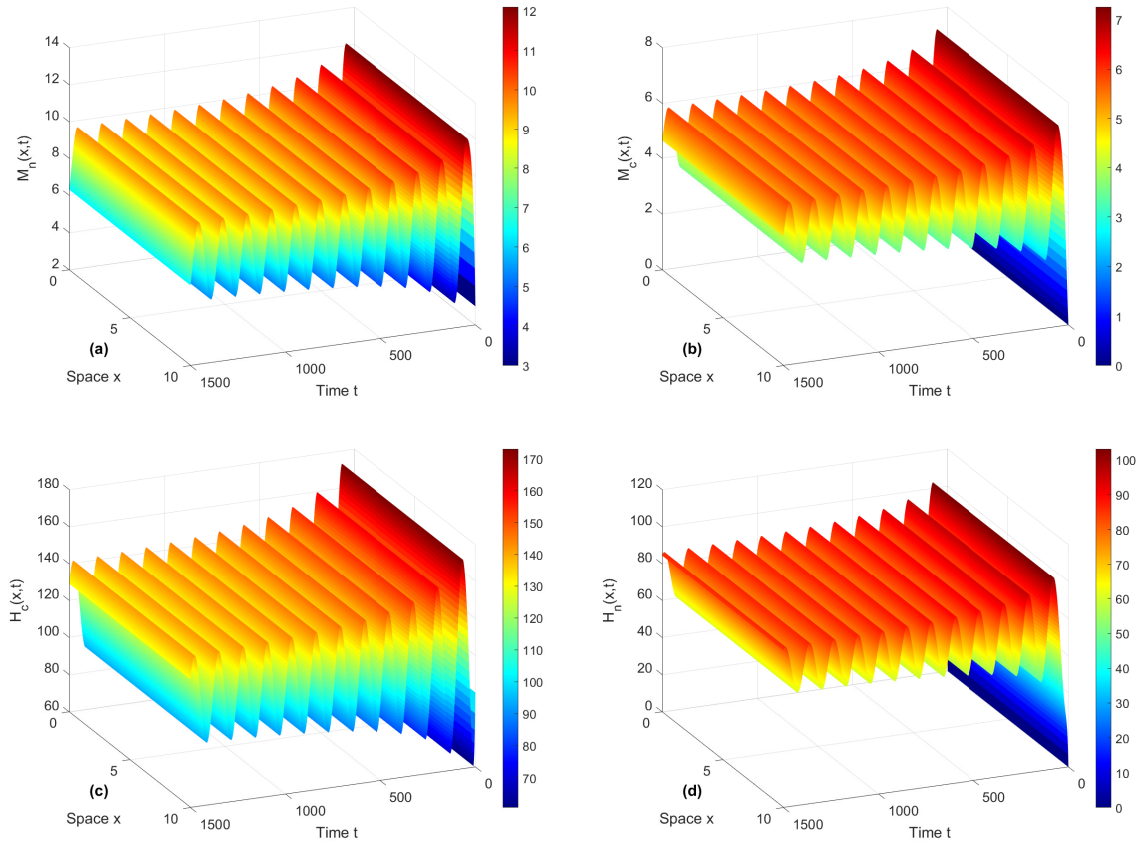

Figure 4. Spatio-temporal simulations for the Hes1 gene expression model (3.5)–(3.8) with delay $\tau = 19 > \tau_0^0$. (a) mRNA concentration in the nucleus, (b) mRNA concentration in the cytoplasm, (c) Hes1 protein concentration in the cytoplasm, and (d) Hes1 protein concentration in the nucleus.

biologically motivated delays, which have been shown in previous studies, including Monk [14], to be critical for sustaining periodic oscillations in Hes1 dynamics. The proposed model (3.5)–(3.8) explicitly incorporates these delays, allowing it to produce oscillations with a period of approximately 2 hours, consistent with experimental observations reported by Hirata et al. [12]. Furthermore, we introduced export and import terms into the model, which were analytically demonstrated in Lemma 2 and numerically validated to be critical for maintaining stable periodic oscillations.

Experimental studies, such as those by Hirata et al. [12], have shown that proteasome inhibition disrupts oscillatory dynamics in the Hes1 system. Specifically, reducing the degradation rate of the Hes1 protein (μ_p) through MG132 treatment suppressed sustained oscillations. Our model successfully reproduces this behavior, showing that a significant reduction in the protein degradation rate disrupts the balance between synthesis and degradation, preventing oscillations. This alignment between experimental and theoretical results underscores the critical role of protein turnover in maintaining oscillatory dynamics and highlights the sensitivity of the system to perturbations in degradation rates.

The numerical simulations provide valuable insights into the model's dynamics near the critical

delay. They demonstrate how small variations in τ can induce qualitative changes in the system's behavior, transitioning from steady-state stability to oscillatory dynamics, a hallmark of Hopf bifurcation. This analysis underscores the importance of the delay parameter τ in regulating the system's dynamic responses, particularly in gene expression networks.

Although the proposed model incorporates both spatial diffusion and transcriptional/translational delays, the numerical simulations presented in this study indicate that the effects of diffusion are minimal, and the behavior of the solutions is predominantly governed by the delay term. Consequently, diffusion does not appear to significantly influence the qualitative dynamics observed in the simulation results. Nevertheless, our theoretical analysis rigorously accounts for diffusion, enabling us to derive conditions under which delay-induced oscillations can arise within a spatially extended framework. Future investigations will aim to explore parameter regimes or biological contexts in which diffusion may play a more pronounced role, as well as to extend the analysis to more complex geometries or coupled multi-species systems.

In conclusion, the present study introduces a novel reaction-diffusion model that combines transcriptional and translational delays, spatial diffusion, and biologically motivated import-export mechanisms, three features not previously integrated into a single framework for Hes1-mRNA dynamics. This unified approach provides an analytically tractable representation of gene regulation that captures essential aspects of observed oscillatory behavior. Beyond its theoretical contributions, the model offers practical relevance by identifying how specific parameters such as delay duration and transport dynamics influence sustained oscillations. These insights can inform experimental strategies aimed at controlling gene expression rhythms in developmental biology and designing synthetic gene circuits with tunable oscillatory behavior.

Use of AI tools declaration

The authors declare they have not used Artificial Intelligence (AI) tools in the creation of this article.

Acknowledgments

This work was supported by the University of Missouri—Kansas City (UMKC) Funding for Excellence Program (2024–2025). Any opinions, findings, conclusions, or recommendations expressed in this material are those of the authors and do not necessarily reflect the views of the university.

Conflict of interest

The authors declare there is no conflict of interest.

References

1. S. K. Bae, Y. Bessho, M. Hojo, R. Kageyama, The bhlh gene Hes6, an inhibitor of Hes1, promotes neuronal differentiation, *Development*, **127** (2000), 2933–2943. https://doi.org/10.1242/dev.127.13.2933

2. R. L. Davis, D. L. Turner, Vertebrate hairy and enhancer of split related proteins: transcriptional repressors regulating cellular differentiation and embryonic patterning, *Oncogene*, **20** (2001), 8342–8357. https://doi.org/10.1038/sj.onc.1205094
3. V. Sriuranpong, M. W. Borges, C. L. Strock, E. K. Nakakura, D. N. Watkins, C. M. Blaumueller, et al., Notch signaling induces rapid degradation of achaete-scute homolog 1, *Mol. Cell. Biol.*, **22** (2002), 3129–3139. https://doi.org/10.1128/MCB.22.9.3129-3139.2002
4. R. Kageyama, T. Ohtsuka, T. Kobayashi, The Hes gene family: repressors and oscillators that orchestrate embryogenesis, *Development*, **134** (2007), 1243–1251. https://doi.org/10.1242/dev.000786
5. T. Kobayashi, R. Kageyama, Expression dynamics and functions of hes factors in development and diseases, *Curr. Top. Dev. Biol.*, **110** (2014), 263–283. https://doi.org/10.1016/B978-0-12-405943-6.00007-5
6. A. Fischer, M. Gessler, Delta–Notch—and then? Protein interactions and proposed modes of repression by Hes and Hey bHLH factors, *Nucleic Acids Res.*, **35** (2007), 4583–4596. https://doi.org/10.1093/nar/gkm477
7. R. Kageyama, T. Ohtsuka, K. Tomita, The bHLH gene Hes1 regulates differentiation of multiple cell types, *Mol. Cells*, **10** (2000), 1–7. https://doi.org/10.1007/s10059-000-0001-0
8. H. Hirata, S. Yoshiura, T. Ohtsuka, Y. Bessho, T. Harada, K. Yoshikawa, et al., Oscillatory expression of the bHLH factor Hes1 regulated by a negative feedback loop, *Science*, **298** (2002), 840–843. https://doi.org/10.1126/science.1074560
9. J. Ross, mRNA stability in mammalian cells, *Microbiol. Rev.*, **59** (1995), 423–450. https://doi.org/10.1128/mr.59.3.423-450.1995
10. L. E. Maquat, G. G. Carmichael, Quality control of mRNA function, *Cell*, **104** (2001), 173–176. https://doi.org/10.1016/S0092-8674(01)00202-1
11. U. Sahin, K. Karikó, Ö. Türeci, mrna-based therapeutics—developing a new class of drugs, *Nat. Rev. Drug Discovery*, **13** (2014), 759–780. https://doi.org/10.1038/nrd4278
12. H. Hirata, S. Yoshiura, T. Ohtsuka, Y. Bessho, T. Harada, K. Yoshikawa, et al., Oscillatory expression of the bHLH factor Hes1 regulated by a negative feedback loop, *Science*, **298** (2002), 840–843. https://doi.org/10.1126/science.1074560
13. M. H. Jensen, K. Sneppen, G. Tiana, Sustained oscillations and time delays in gene expression of protein Hes1, *FEBS Lett.*, **541** (2003), 176–177. https://doi.org/10.1016/S0014-5793(03)00279-5
14. N. A. M. Monk, Oscillatory expression of Hes1, p53, and NF-kB driven by transcriptional time delays, *Curr. Biol.*, **13** (2003), 1409–1413. https://doi.org/10.1016/S0960-9822(03)00494-9
15. M. Santillán, On the use of the hill functions in mathematical modelsof gene regulatory networks, *Math. Modell. Nat. Phenom.*, **3** (2008), 85–97. https://doi.org/10.1051/mmnp:2008056
16. S. Bernard, B. Čajavec, L. Pujo-Menjouet, L. Mackey, H. Herzel, Modelling transcriptional feedback loops: the role of Gro/TLE1 in Hes1 oscillations, *Philos. Trans. R. Soc. London, Ser. A*, **364** (2006), 1155–1170. https://doi.org/10.1098/rsta.2006.1761
17. K. Rateitschak, O. Wolkenhauer, Intracellular delay limits cyclic changes in gene expression, *Math. Biosci.*, **205** (2007), 163–179. https://doi.org/10.1016/j.mbs.2006.08.010

18. H. Momiji, N. A. M. Monk, Dissecting the dynamics of the Hes1 genetic oscillator, *J. Theor. Biol.*, **254** (2008), 784–798. https://doi.org/10.1016/j.jtbi.2008.07.013

19. D. Kasinathan, D. Chalishajar, R. Kasinathan, R. Kasinathan, S. Karthikeyan, Trajectory controllability of higher-order fractional neutral stochastic system with non-instantaneous impulses via state-dependent delay with numerical simulation followed by hearth wall degradation process, *Int. J. Dyn. Control*, **13** (2025), 104. https://doi.org/10.1007/s40435-025-01605-w

20. D. Kasinathan, R. Kasinathan, R. Kasinathan, D. Chalishajar, Exponential stability for higher-order impulsive fractional neutral stochastic integro-delay differential equations with mixed brownian motions and non-local conditions, *Int. J. Optim. Control Theor. Appl.*, **15** (2025), 103–122. https://doi.org/10.36922/ijocta.1524

21. D. N. Chalishajar, D. Kasinathan, R. Kasinathan, R. Kasinathan, Exponential stability of higher order fractional neutral stochastic differential equation via integral contractors, *Math. Methods Appl. Sci.*, in press.

22. Y. Chi, Y. Dong, L. Zhang, Z. Qiu, X. Zheng, Z. Li, Collaborative control of UAV swarms for target capture based on intelligent control theory, *Mathematics*, **13** (2025), 413. https://doi.org/10.3390/math13030413

23. M. Sturrock, A. J. Terry, D. P. Xirodimas, A. M. Thompson, M. A. J. Chaplain, Spatio-temporal modelling of the Hes1 and p53-Mdm2 intracellular signalling pathways, *J. Theor. Biol.*, **273** (2011), 15–31. https://doi.org/10.1016/j.jtbi.2010.12.016

24. Y. Zhang, J. Cao, L. Liu, H. Liu, Z. Li, Complex role of time delay in dynamical coordination of neural progenitor fate decisions mediated by notch pathway, *Chaos, Solitons Fractals*, **180** (2024), 114479. https://doi.org/10.1016/j.chaos.2024.114479

25. A. Giri, S. Kar, Deciphering the impact of pulsatile input in the population-level synchrony of the Hes1 oscillators, *J. Chem. Sci.*, **135** (2023), 71. https://doi.org/10.1007/s12039-023-02177-y

26. A. Rowntree, N. Sabherwal, N. Papalopulu, Bilateral feedback in oscillator model is required to explain the coupling dynamics of Hes1 with the cell cycle, *Mathematics*, **10** (2022), 2323. https://doi.org/10.3390/math10132323

27. S. N. Singh, M. Z. Malik, R. K. B. Singh, Molecular crosstalk: Notch can manipulate Hes1 and miR-9 behavior, *J. Theor. Biol.*, **504** (2020), 110404. https://doi.org/10.1016/j.jtbi.2020.110404

28. T. Iwasaki, R. Takiguchi, T. Hiraiwa, T. G. Yamada, K. Yamazaki, N. F. Hiroi, et al., Neural differentiation dynamics controlled by multiple feedback loops in a comprehensive molecular interaction network, *Processes*, **8** (2020), 166. https://doi.org/10.3390/pr8020166

29. M. Boareto, D. Iber, V. Taylor, Differential interactions between Notch and ID factors control neurogenesis by modulating Hes factor autoregulation, *Development*, **144** (2017), 3465–3474. https://doi.org/10.1242/dev.152520

30. S. Li, Y. Liu, Z. Liu, R. Wang, Neural fate decisions mediated by combinatorial regulation of Hes1 and miR-9, *J. Biol. Phys.*, **42** (2016), 53–68. https://doi.org/10.1111/j.1728-4457.2016.00107.x

31. H. Wang, Y. Huang, L. Zheng, Y. Bao, L. G. Sun, Y. Wu, et al., Modelling coupled oscillations in the Notch, Wnt, and FGF signaling pathways during somitogenesis: a comprehensive mathematical model, *Comput. Intell. Neurosci.*, **2015** (2015), 387409. https://doi.org/10.1155/2015/387409

32. M. Sturrock, A. Hellander, S. Aldakheel, L. Petzold, M. A. J. Chaplain, The role of dimerisation and nuclear transport in the Hes1 gene regulatory network, *Bull. Math. Biol.*, **76** (2014), 766–798. https://doi.org/10.1007/s11538-013-9842-5
33. S. Li, Z. Liu, R. Wang, Neural fate decisions mediated by oscillatory and sustained Hes1, in *Proceedings of the 2014 8th International Conference on Systems Biology (ISB)*, IEEE, (2014), 189–193. https://doi.org/10.1109/ISB.2014.6990754
34. A. Barton, A. J. Fendrik, Sustained vs. oscillating expressions of Ngn2, Dll1 and Hes1: a model of neural differentiation of embryonic telencephalon, *J. Theor. Biol.*, **328** (2013), 1–8. https://doi.org/10.1016/j.jtbi.2013.03.004
35. M. Sturrock, A. J. Terry, D. P. Xirodimas, A. M. Thompson, M. A. J. Chaplain, Influence of the nuclear membrane, active transport, and cell shape on the Hes1 and p53–Mdm2 pathways: insights from spatio-temporal modelling, *Bull. Math. Biol.*, **74** (2012), 1531–1579. https://doi.org/10.1007/s11538-012-9725-1
36. M. A. Tabatabai, W. M. Eby, Z. Bursac, Oscillabolastic model, a new model for oscillatory dynamics, applied to the analysis of Hes1 gene expression and Ehrlich ascites tumor growth, *J. Biomed. Inf.*, **45** (2012), 401–407. https://doi.org/10.1162/LEON_a_00435
37. M. Bani-Yaghoub, D. E. Amundsen, Dynamics of notch activity in a model of interacting signaling pathways, *Bull. Math. Biol.*, **72** (2010), 780–804. https://doi.org/10.1007/s11538-009-9469-8
38. M. Bani-Yaghoub, D. E. Amundsen, The role of Retinoic Acid and Notch in the symmetry breaking instabilities for axon formation, in *International Conference on Mathematical Biology, World Scientific and Engineering Academy and Society (WSEAS)*, 2006.
39. M. Bani-Yaghoub, D. E. Amundsen, Turing-type instabilities in a mathematical model of notch and retinoic acid pathways, 2006.
40. M. Bani-Yaghoub, Analysis and applications of delay differential equations in biology and medicine, preprint, arXiv:1701.04173.
41. M. Bani-Yaghoub, Introduction to delay models and their wave solutions, preprint, arXiv:1701.04703.
42. M. Bani-Yaghoub, C. Ou, G. Yao, Delay-induced instabilities of stationary solutions in a single species nonlocal hyperbolic-parabolic population model, *Discrete Contin. Dyn. Syst. - Ser. S*, **13** (2020), 2509–2535. https://doi.org/10.3934/dcdss.2020195
43. K. Gopalsamy, *Stability and Oscillations in Delay Differential Equations of Population Dynamics*, Kluwer Academic Publishers, Dordrecht, Netherlands, 1992.
44. Y. Zhang, H. Liu, F. Yan, J. Zhou, Oscillatory behaviors in genetic regulatory networks mediated by microrna with time delays and reaction-diffusion terms, *IEEE Trans. Nanobiosci.*, **16** (2017), 166–176. https://doi.org/10.1109/TNB.2017.2675446
45. X. Wang, A simple proof of descartes's rule of signs, *Am. Math. Mon.*, **111** (2004), 525–526. https://doi.org/10.1080/00029890.2004.11920108
46. S. Ruan, J. Wei, On the zeros of transcendental functions with applications to stability of delay differential equations with two delays, *Dyn. Contin. Discrete Impulsive Syst. Ser. A*, **10** (2003), 863–874.

47. T. Dong, X. Liao, A. Wang, Stability and Hopf bifurcation of a complex-valued neural network with two time delays, *Nonlinear Dyn.*, **82** (2015), 173–184. https://doi.org/10.1007/s11071-015-2147-5

48. T. Dong, Q. Zhang, Stability and oscillation analysis of a gene regulatory network with multiple time delays and diffusion rate, *IEEE Trans. Nanobiosci.*, **19** (2020), 285–298. https://doi.org/10.1109/TNB.2020.2964900

49. J. K. Hale, *Theory of Functional Differential Equations*, *Applied Mathematical Sciences*, Springer, 2012.

50. A. Verdugo, R. Rand, Hopf bifurcation in a DDE model of gene expression, *Commun. Nonlinear Sci. Numer. Simul.*, **13** (2008), 235–242. https://doi.org/10.3998/ark.5550190.0009.225

AIMS Press